

On the width of the monotone-visibility kernel of a simple polygon

David Orden¹, Leonidas Palios², Carlos Seara³, Jorge Urrutia⁴, and Paweł Żyliński⁵

- 1 Departamento de Física y Matemáticas, Universidad de Alcalá, Spain, david.orden@uah.es
- 2 Dept. of Computer Science and Engineering, University of Ioannina, Greece, palios@cs.uoi.gr
- 3 Mathematics Department, Universitat Politècnica de Catalunya, Spain, carlos.seara@upc.edu
- 4 Instituto de Matemáticas, Universidad Nacional Autónoma de México, México, urrutia@matem.unam.mx
- 5 Institute of Informatics, University of Gdańsk, Poland, zyliniski@inf.ug.edu.pl

Abstract

Given a simple polygonal region P with n vertices, we present an efficient $O(n \log n)$ time and $O(n)$ space algorithm for computing, over all values of angle θ , the maximum width of the θ -kernel(P), i.e., the locus of points in P from which any point of P can be reached by a $(\theta + \frac{\pi}{2})$ -monotone path.

1 Introduction

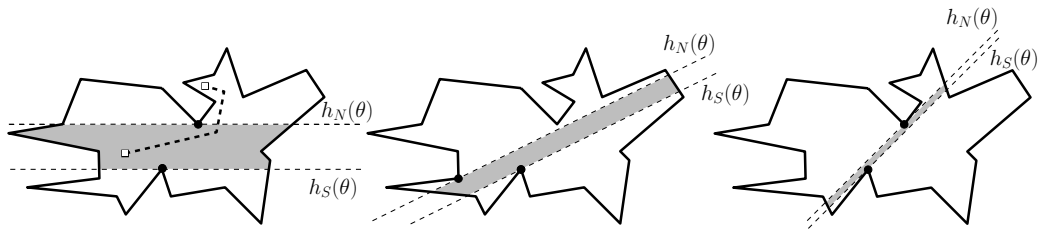
The computation of the *widest corridor through a set S of n points* in the plane, defined as an open region bounded by two parallel lines that intersect the convex hull of S , has attracted the interest of the computational geometry community since the late 1980s and early 1990s, having applications to robot motion planning [2, 4, 5]. Computing the *width of a simple polygon P with n vertices*, defined as the width of the narrowest corridor containing P , is another well-known problem in computational geometry [8]; it can be computed in linear time using what are known as rotating calipers [10].

The present work deals with the width of a particular corridor through a simple polygonal region P : the θ -kernel of P , denoted as θ -kernel(P). The θ -kernel(P) is defined as the locus of points in P from which any point of P can be reached by a path which has a connected intersection with any line forming an angle θ with the positive x -axis or, in other words, which is monotone with respect to the direction $\theta + \frac{\pi}{2}$. Figure 1 shows the θ -kernel of a polygon for three different values of the angle θ , together with an example of a $\frac{\pi}{2}$ -monotone path from a point inside the 0-kernel. For further details see [6]. We present an efficient $O(n \log n)$ time and $O(n)$ space algorithm that, given a simple polygonal region P with n vertices, finds an angle $\theta \in [-\frac{\pi}{2}, \frac{\pi}{2})$ for which the width of the θ -kernel(P) is maximized.



This work has received funding from the European Union's Horizon 2020 research and innovation programme under the Marie Skłodowska-Curie grant agreement No 734922.

13:2 On the width of the monotone-visibility kernel of a simple polygon

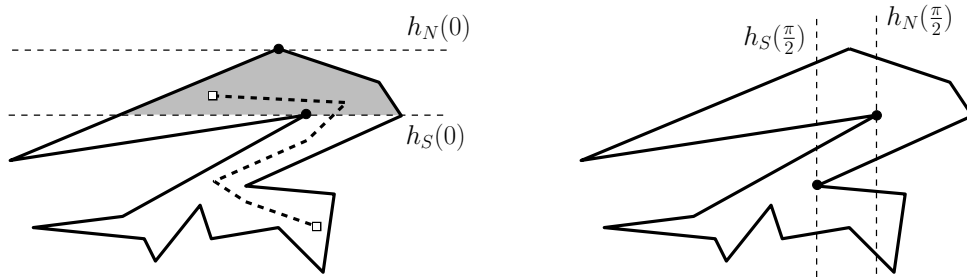


■ **Figure 1** The θ -kernel(P) is shaded for $\theta = 0$ (left), for $\theta = \frac{\pi}{8}$ (middle), and for $\theta = \frac{\pi}{4}$ (right). In addition, a vertically monotone path from a point inside the 0-kernel is shown.

In the following we assume that the vertices of P are labeled $\{p_1, p_2, \dots, p_n\}$ in counter-clockwise order around the boundary of P and that a θ -orientation will be an oriented line forming angle θ with the x -axis.

► **Definition 1.1.** A reflex vertex $p_i \in P$ such that p_{i-1} and p_{i+1} are both below (resp. above) p_i with respect to a given θ -orientation is a *reflex maximum* (resp. *reflex minimum*) with respect to the θ -orientation. An edge with orientation θ such that its two neighbors are below (resp. above) with respect to that θ -orientation is also a reflex maximum (resp. minimum) edge with respect to the θ -orientation.

For a given θ -orientation, P can have several reflex minima and reflex maxima, so there is a lowest reflex minimum and a highest reflex maximum with respect to θ . It may also happen that P has no reflex maxima (resp. minima), and then the role of the highest reflex maximum (resp. lowest reflex minimum) will be undertaken by the lowest (resp. highest) vertex of P . See Figure 2, left.



■ **Figure 2** Left: The shaded area is the 0-kernel of a polygonal region P , where the role of the lowest reflex minimum is undertaken by the highest vertex of P . A vertically monotone path from a point in the kernel is also shown. Right: The $\frac{\pi}{2}$ -kernel of the same P turns out to be empty.

► **Definition 1.2.** A pair (p, q) of vertices of P forms a *pair of antipodal interior vertices* of P for a θ -orientation if p is the lowest reflex minimum vertex and q is the highest reflex maximum vertex with respect to the θ -orientation, or vice versa.

In Figure 1 the pair of antipodal points is the same for $\theta = 0$ (left) and $\theta = \frac{\pi}{4}$ (right), although the pair has changed in between for $\theta = \frac{\pi}{8}$ (middle). Let $h_N(\theta)$ and $h_S(\theta)$ be, respectively, the θ -orientations passing through the lowest reflex minimum and the highest reflex maximum with respect to the current θ -orientation.

► **Lemma 1.3** ([9]). *The θ -kernel(P) is empty when $h_N(\theta)$ is below $h_S(\theta)$ with respect to θ . Otherwise, it is given by the intersection of P and the strip determined by $h_N(\theta)$ and $h_S(\theta)$.*

Figure 2, right, shows an example where the $\frac{\pi}{2}$ -kernel(P) is empty because, with respect to the $\frac{\pi}{2}$ -orientation, $h_N(\frac{\pi}{2})$ is below (to the right of) $h_S(\frac{\pi}{2})$. That is, there is no point from which all other points could be reached by a horizontally monotone path.

In order to compute the maximum width of the θ -kernel(P) we maintain the lines $h_N(\theta)$ and $h_S(\theta)$ enclosing the θ -kernel(P) for $\theta \in [-\frac{\pi}{2}, \frac{\pi}{2})$. As the pairs of antipodal interior vertices of P can change during the process, we subdivide $[-\frac{\pi}{2}, \frac{\pi}{2})$ into subintervals $[\theta_i, \theta_{i+1})$ where the pair of antipodal interior vertices does not change, so that it is enough to compute the maximum value of the width of the θ -kernel(P) for θ in each of these subintervals $[\theta_i, \theta_{i+1})$.

2 Computing the maximum width of the θ -kernel(P)

Next, we sketch the algorithm to compute the intervals of the values of θ within $[-\frac{\pi}{2}, \frac{\pi}{2})$ such that θ -kernel(P) $\neq \emptyset$; i.e., the width of the θ -kernel(P), is not zero. Then we calculate the maximum width, and maintain its maximum value over all the intervals.

ALGORITHM FOR COMPUTING INTERVALS SUCH THAT θ -kernel(P) $\neq \emptyset$

1. For each vertex $p_i \in P$, check whether p_i is reflex. If it is, compute the angular intervals $[\theta_1^i, \theta_2^i)$ and $[\theta_1^i + \pi, \theta_2^i + \pi)$ of orientations θ for which p_i is reflex, and the corresponding *reflex slope intervals* defined when rotating with pivot p_i the line containing the edge $p_{i-1}p_i$ up to the line containing the edge $p_i p_{i+1}$ (see Figure 3, left). Then the vertex p_i is a candidate to be a reflex maximum and a reflex minimum only for the θ -orientations in those reflex slope intervals. Note that, since $\theta \in [-\frac{\pi}{2}, \frac{\pi}{2})$, a reflex slope interval may be split into two if it contains the orientation $\pi/2$.
2. Compute the sequence of *event intervals*, $[\theta_i, \theta_{i+1}) \subset [-\frac{\pi}{2}, \frac{\pi}{2})$, each one defined by a pair of θ -orientations such that for any value $\theta \in [\theta_i, \theta_{i+1})$, the strip θ -kernel(P) is supported by the same pair of reflex vertices; i.e., the same lowest reflex minimum and highest reflex maximum for any $\theta \in [\theta_i, \theta_{i+1})$. See Figure 1. The strip θ -kernel(P) with θ -orientation is empty if the lowest reflex minimum is below the highest reflex maximum. In order to compute the sequence of event intervals do the following:

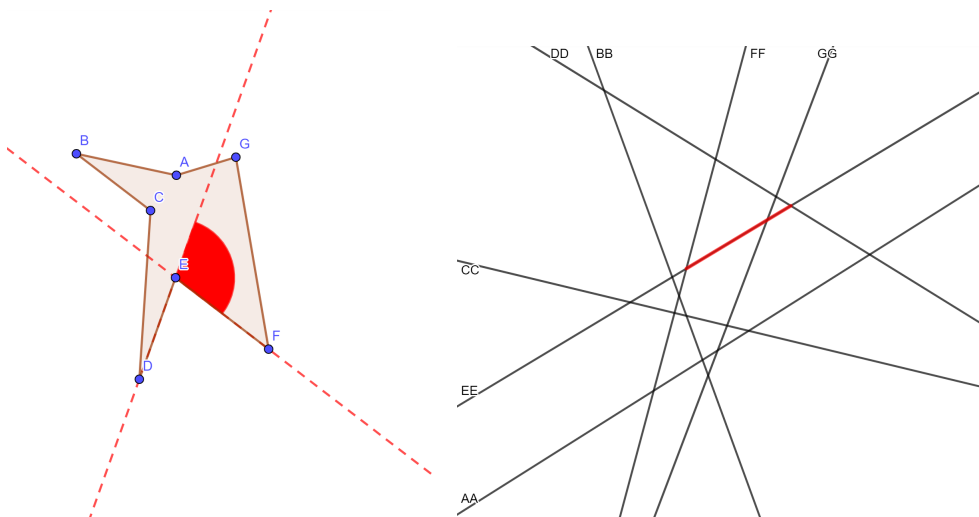


Figure 3 Dualization of vertices into lines and a reflex slope interval into a segment.

13:4 On the width of the monotone-visibility kernel of a simple polygon

- a. Dualize the vertices $p_i \in P$ into lines $D(p_i)$. On each of these lines, mark the segment corresponding to the reflex slope interval of its primal point; i.e., dualize the supporting lines on p_i with slopes in those intervals. See Figure 3.

Color the segment blue if it corresponds to a reflex minimum vertex or red if it corresponds to a reflex maximum vertex. Note that since a reflex vertex can become reflex minimum for a θ -orientation and reflex maximum for the $(\theta + \pi)$ -orientation, corresponding blue and red segments can lie on the same dual line corresponding to that vertex.

It may be the case that for some θ -orientations there are no reflex minimum or no reflex maximum vertices because there are no reflex vertices at all; i.e., at those θ -orientations P has a convex chain part, and then the lowest or the highest convex vertices of $CH(P)$ play the role of the lowest reflex minimum or the highest reflex maximum for those θ -orientations. Then we mark the line segments in the dual accordingly, corresponding to those convex chains of $CH(P)$; i.e., red if there is no reflex minimum or blue if there is no reflex maximum.

- b. Let \mathcal{D}_R and \mathcal{D}_B be the arrangements containing the blue and red segments defined above. We then do a line-sweep with a vertical line (corresponding to a value θ) from left to right such that the vertical line intersects some segments of the arrangement, which correspond to the reflex vertices in the primal. Since dualization preserves the above–below relationships between lines and/or points, the lowest blue segment and the highest red segment intersected by the vertical line in the dual correspond to the lowest reflex minimum and to the highest reflex maximum in the primal.

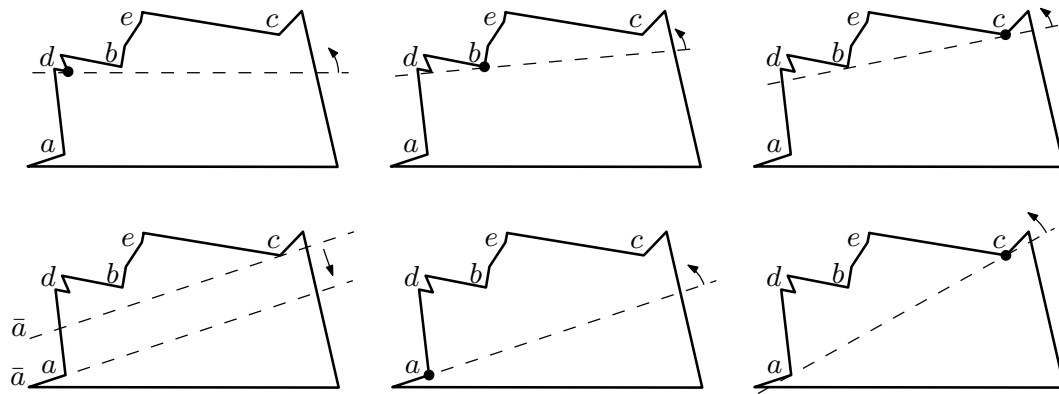
3. To do the line-sweep of step 2 in $O(n \log n)$ time, we compute the lower envelope of \mathcal{D}_B , $\mathcal{L}_{\mathcal{D}_B}$ and the upper envelope of \mathcal{D}_R , $\mathcal{U}_{\mathcal{D}_R}$ [3]. After merging the two envelopes in linear time, we do a line-sweep of $\mathcal{L}_{\mathcal{D}_B} \cup \mathcal{U}_{\mathcal{D}_R}$, obtaining the sequence of pairs of antipodal interior points for all the *event intervals* $[\theta_i, \theta_{i+1}]$ as θ varies in $[-\frac{\pi}{2}, \frac{\pi}{2}]$.

In general, the lower envelope and the upper envelope of a set of n (possibly intersecting) line segments in the plane have worst-case size $O(n\alpha(n))$, where $\alpha(n)$ is the extremely–slowly–growing inverse of Ackermann’s function [1], which would consequently give that the number of pairs of antipodal interior vertices is $O(n\alpha(n))$; see [3]. However, for this particular arrangement of segments, we can prove that the complexity of the lower envelope $\mathcal{L}_{\mathcal{D}_B}$ and of the upper envelope $\mathcal{U}_{\mathcal{D}_R}$ are in $O(n)$. For the sake of easier reading, this claim is proved as Lemma 2.1 below. Thus, merging the two envelopes has $O(n)$ complexity and we can line-sweep them in linear time.

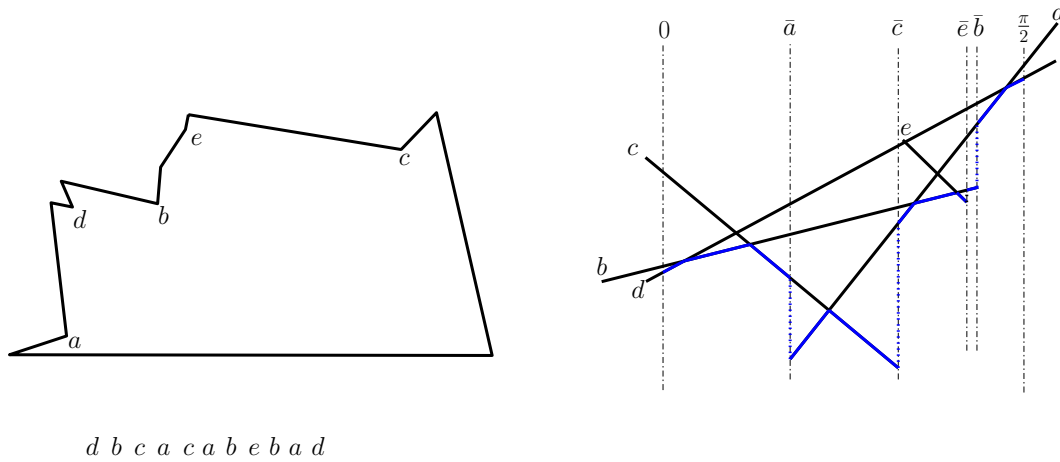
4. Update an *event interval* $[\theta_i, \theta_{i+1}] \subseteq [-\frac{\pi}{2}, \frac{\pi}{2}]$ if, for the corresponding pair, the lowest reflex minimum is above the highest reflex maximum in a θ -orientation.

► **Lemma 2.1.** *The complexity of the lower envelope $\mathcal{L}_{\mathcal{D}_B}$ and the complexity of the upper envelope $\mathcal{U}_{\mathcal{D}_R}$ are in $O(n)$.*

Proof. Clearly, the proof for the complexity of the lower envelope $\mathcal{L}_{\mathcal{D}_B}$ is analogous to the proof for the complexity of the upper envelope $\mathcal{U}_{\mathcal{D}_R}$. Thus, we concentrate on the former. Figure 4 shows an example where the lowest reflex minimum for $\theta_1 = 0$ is d , and increasing θ gives rise to a counterclockwise sliding rotation [7]; rotating with pivot at d , we hit b and change the pivot to it, then hit c and change the pivot to it. When θ reaches the orientation \bar{a} aligned to an edge incident to a , a becomes a reflex minimum, so we slide to a , then pivot around a , until we hit c , and so on. Figure 5 shows the primal on the left, including the full sequence of pivots, and the dual on the right, including the lower envelope $\mathcal{L}_{\mathcal{D}_B}$.



■ **Figure 4** From left to right and from top to bottom, first steps of a sliding rotation. The pivot point at each step is marked.



■ **Figure 5** Left: Full sequence of pivots for the polygonal region in Figure 4 (where only the first five pivots were included). Right: Illustration of the dual and the lower envelope $\mathcal{L}_{\mathcal{D}_B}$.

Next, for the rotation between 0 and $\frac{\pi}{2}$, we describe a charging scheme proving that the complexity of $\mathcal{L}_{\mathcal{D}_B}$ is in $O(n)$ (an analogous argument holds for the rest of the rotation and for $\mathcal{U}_{\mathcal{D}_R}$). Figure 6, left, shows in purple the *interior tangents*, when a vertex is hit by the rotation motion, together with an auxiliary dashed horizontal tangent arriving at the starting vertex d . Figure 6, right, shows the dual, the lower envelope $\mathcal{L}_{\mathcal{D}_B}$, and the charging labels in blue.

1. When a vertex z is reached by a sliding motion, this is because the orientation has aligned with a side of the polygon incident to the vertex y . In this case, the vertex z receives the label \bar{y} (the bar indicating “side incident to”). Note that this may happen either (i) because z was *inactive* (not reflex minimum) and it becomes *active* (reflex minimum), like the first appearance of a in Figure 6 where $y = a$ and hence the label is \bar{a}); or (ii) because an active vertex becomes inactive, like the second appearance of c in Figure 6, and the sliding motion hits z (in the figure, this z is the second appearance of a , which is labeled as \bar{c} because in this case $y = c$).
2. When a vertex z is hit by a rotating motion, an interior tangent yz arises.
 - a. If this is the first appearance of z , it receives the label z .

13:6 On the width of the monotone-visibility kernel of a simple polygon

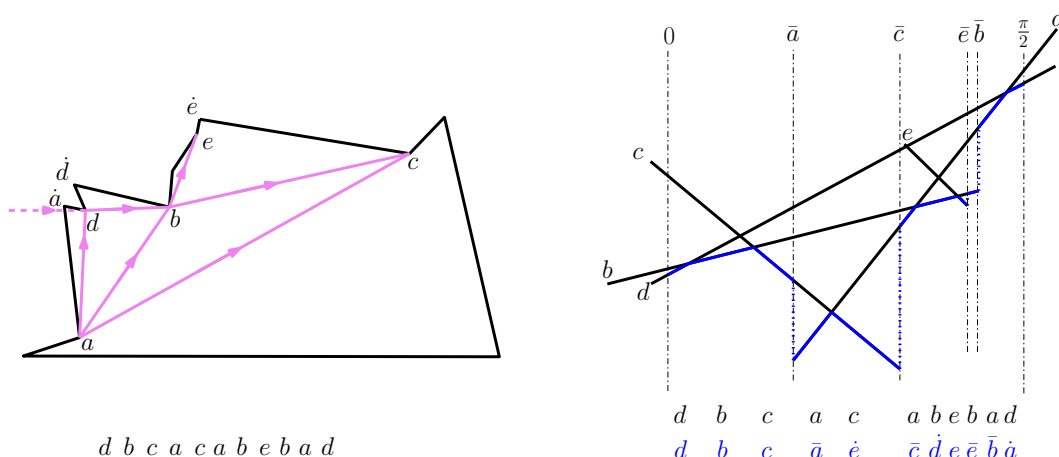


Figure 6 Left: Polygon, sequence of vertices, and interior tangents. Right: Dual and charging labels.

- b. If this z has already been hit, then it is charged to the convex vertex \dot{r} closest to z in CCW order that has not already been used (in the figure, the second appearance of c is charged to \dot{e} , with the dot indicating “convex vertex incident to”).

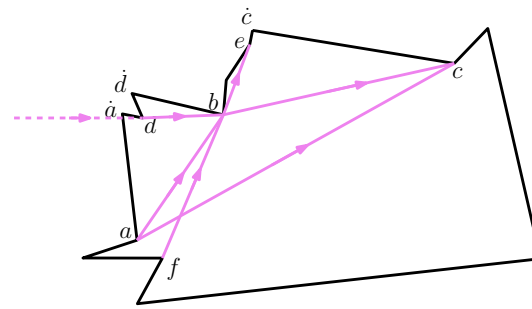
It is clear that a label \bar{z} can appear at most two times and that a label z can appear at most once. In order to see that a label \dot{r} always exists, observe that for z to have been hit before yz , a tangent xz with $\text{slope}(xz) < \text{slope}(yz)$ must exist. Hence, z being reflex at orientation yz and y being reflex at orientation yz imply that there is a convex vertex \dot{r} above yz , where r is the closest reflex vertex to \dot{r} in CCW order. For an example, take $z = b, y = a, x = d, r = d$ in Figure 6, where the second appearance of b happens at a tangent ab and there is a tangent db with $\text{slope}(db) < \text{slope}(ab)$, so that a convex vertex \dot{d} exists above db . The same happens for $z = c, y = a, x = b, r = e$ and for $z = d, y = a, x = \text{horizontal}$, and $r = a$, using the auxiliary dashed horizontal arriving at d in order to label the last d in the sequence as \dot{a} . (See Figure 7 for a second example.)

It just remains to show that for each y , a \dot{y} is used only once. To this end, observe that a quadruple of internal tangents xz, yz, xt , and yt cannot appear: Without loss of generality, assume that the extensions of xt and yz do cross when extending from x and y as in the figure. Then, xt is not a valid interior tangent, since f is a lower reflex vertex. See Figure 8, where $z = b, y = f, x = a$, and $t = u$. ◀

By Lemma 2.1, the sizes of both the lower envelope and the upper envelope are linear, so all the steps of the algorithm above can be done within $O(n \log n)$ time and $O(n)$ space. Therefore, we get the following result.

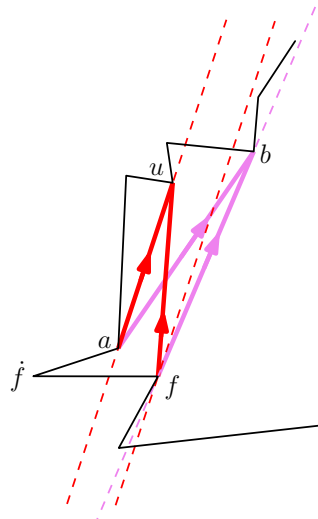
► **Theorem 2.2.** For a simple polygon P with n vertices, there are $O(n)$ angular intervals $[\theta_i, \theta_{i+1}) \subset [-\frac{\pi}{2}, \frac{\pi}{2})$ such that θ -kernel(P) $\neq \emptyset$ for all the values $\theta \in (\theta_i, \theta_{i+1})$, and the set of such intervals together with the maximum value of the width of the θ -kernel(P) can be computed and maintained in $O(n \log n)$ time and $O(n)$ space.

Proof. For each of the $O(n)$ angular intervals, compute the maximum value of the width of the θ -kernel(P) for $\theta \in [\theta_i, \theta_{i+1})$ in constant time since we know the pair of supporting points, the range of the value θ , and that the width of the θ -kernel(P) is an unimodal function. ◀



$db c a c a b f b e b f$
 $db c \bar{a} \bar{c} \bar{c} \dot{d} \dot{f} \hat{a} e \bar{e} \bar{b}$

■ **Figure 7** Another example of the charging scheme.



■ **Figure 8** Illustration of why label \dot{f} is not used a second time.

► **Corollary 2.3.** *The maximum width of the θ -kernel(P) simple polygon P with n vertices can be computed in $O(n \log n)$ time and $O(n)$ space.*

Acknowledgements

David Orden was supported by project MTM2017-83750-P of the Spanish Ministry of Science (AEI/FEDER, UE). Carlos Seara was supported by projects MTM2015-63791-R MINECO/FEDER and Gen. Cat. DGR 2017SGR1640. Jorge Urrutia was supported in part by SEP-CONACYT of Mexico, Proyecto 80268, and by PAPIIT IN102117 Programa de Apoyo a la Investigación e Innovación Tecnológica, UNAM. Paweł Żyliński was supported by the grant 2015/17/B/ST6/01887 (National Science Centre, Poland).

References

- 1 W. Ackermann. Zum Hilbertschen Aufbau der reellen Zahlen. *Mathematische Annalen*, 99, (1928), 118–133.

- Canadian Conference on Computational Geometry*, (2001).
- 2 S. Chattopadhyay and P. Das. The k -dense corridor problems. *Pattern Recognition Letters*, 11, (1990), 463–469.
 - 3 J. Hershberger. Finding the upper envelope of n line segments in $O(n \log n)$ time. *Inf. Process. Lett.*, 33(4), (1989), 169–174.
 - 4 M. Houle and A. Maciel. Finding the widest empty corridor through a set of points. In *G.T. Toussaint, editor, Snapshots of Computational and Discrete Geometry*, 201–213. TR SOCS-88.11, Dept. of Computer Science, McGill University, Montreal, Canada, (1988).
 - 5 R. Janardan and F. P. Preparata. Widest-corridor problems. *Nordic Journal of Computing*, 1, (1994), 231–245.
 - 6 D. Orden, L. Palios, C. Seara, and P. Żyliński. Generalized kernels of polygons under rotation. In *Proceedings of EuroCG 2018*, paper 74.
 - 7 D. Orden, P. Ramos, and G. Salazar. The number of generalized balanced lines. *Discrete & Computational Geometry*, 44(4), 2010, 805–811.
 - 8 F. P. Preparata and M. I. Shamos. *Computational Geometry: An introduction*, Springer-Verlag, (1985).
 - 9 S. Schuierer, G. J. E. Rawlins, and D. Wood. A generalization of staircase visibility. *3rd Canadian Conference on Computational Geometry*, Vancouver, 1991, 96–99.
 - 10 G. Toussaint. Solving geometric problems with the rotating calipers. In *Proceedings of IEEE MELECON'83*, Athens, Greece, May 1983.